J Mol Model (2015) 21: 195
DOI 10.1007/s00894-015-2726-x

ORIGINAL PAPER

# A density functional theory study of CO oxidation on $CuO_{1-x}(111)$

**Bing-Xing Yang [1,2,4] · Li-Ping Ye [1,2] · Hui-Jie Gu [1,2] · Jin-Hua Huang [1,2] · Hui-Ying Li [3] · Yong Luo [1,2]**

Received: 6 April 2015 / Accepted: 8 June 2015 / Published online: 12 July 2015


**Abstract** The surface structures, CO adsorption, and oxidation-reaction properties of $CuO_{1-x}(111)$ with different reduction degree have been investigated by using density functional theory including on-site Coulomb corrections (DFT+U). Results indicate that the reduction of Cu has a great influence on the adsorption of CO. Electron localization caused by the reduction turns $Cu^{2+}$ to $Cu^{+}$, which interacts much stronger with CO, and the adsorption strength of CO is related to the electronic interaction with the substrate as well as the structural relaxation. In particular, the electronic interaction is proved to be the decisive factor. The surfaces of $CuO_{1-x}(111)$ with different reduction degree all have good adsorption to CO. With the expansion of the surface reduction degree, the amount of CO that is stably adsorbed on the surface increases, while the number of surface active lattice O decreases. In general, the activity of CO oxidation first rises and then declines.

**Keywords** CO adsorption · CuO · DFT · Surface reduction

**Electronic supplementary material** The online version of this article (doi:10.1007/s00894-015-2726-x) contains supplementary material, which is available to authorized users.

✉ Yong Luo
luoyongno.1@163.com

[1] Shanghai Research Institute of Chemical Industry, Shanghai 200062, People's Republic of China

[2] Shanghai Key Laboratory of Catalysis Technology for Polyolefins, Shanghai 200062, People's Republic of China

[3] Shanghai Institute of Technology, Shanghai 200235, People's Republic of China

[4] Centre for Computational Chemistry, East China University of Science and Technology, Shanghai 200237, People's Republic of China

## Introduction

Transition metal oxides have a wide application in CO oxidation [1–3]. Among them, CuO based catalysts have been given much more attention for their low price and high activity [4–7], which is roughly the same or superior to that of catalysts based on noble metals, especially in low-temperature CO oxidation [8–10].

For CuO based catalysts, most studies were focused on the roles of dopant atoms and interfaces between CuO and the support [11–13]. Luo and Lu and their co-workers [14] investigated the synergetic effects and kinetic study of CO oxidation over $CuO/Ce_{1-x}Cu_xO_{2-\delta}$ and $Ce_{1-x}Cu_xO_{2-\delta}$ catalysts. Kinetic studies showed that the apparent activation energy was 42 $kJ \cdot mol^{-1}$ for $CuO/Ce_{1-x}Cu_xO_{2-\delta}$ and 95 $kJ \cdot mol^{-1}$ for $Ce_{1-x}Cu_xO_{2-\delta}$. They confirmed that the surface CuO particles provide sites for CO chemisorption and the $Ce_{1-x}Cu_xO_{2-\delta}$ solid solution promotes the activation of oxygen. Moreover, they also proposed that the adsorption peak at 2110 $cm^{-1}$ attributed to chemisorbed CO over $Cu^{+}$ ion, which was also suggested by Martínez-Arias et al. [11]. In fact, in recent years, there is more and more experimental evidence that points to the crucial role played by $Cu^{+}$ ion in CO oxidation [15, 16]. Wan et al. [17] studied the CO oxidation activities of $CuO/\gamma\text{-}Al_2O_3$ catalysts, proposing that dispersed $Cu^{+}$ species played a significant role in low-temperature CO oxidation (≤200 °C). They also suggested that CO-$Cu^{+}$ interaction was much stronger than those of CO-$Cu^{2+}$ and CO-$Cu^{0}$. In our previous experimental studies, we found that CuO based catalysts with a certain degree of reduction (70 ~80 %) showed a very high activity for CO oxidation compared to the pure and other catalysts with different reduction degrees [18].

Theoretical simulations based on first principle calculations have been carried out to explore the stabilities, electronic structures, and surface activities of CuO surfaces [19–22]. Wang et al. [21] studied the two elementary reactions: CO+

*→CO* and CO*+$O_{latt}$→$CO_2$+$O_{vac}$ over several metal oxide surfaces. They found that on CuO(111) surface, the reaction barrier for CO*+$O_{latt}$→$CO_2$+$O_{vac}$ was very low. However, CO adsorption was relatively weak (0.74 eV), giving rise to the overall low activity at low temperature. Several reports also suggested that the adsorption of CO was quite weak on the CuO surfaces [19, 23]. Nevertheless, investigations of the surface structural properties and CO oxidation of reduced CuO surface are still rather limited.

CuO(111) surface was considered to be the most stable surface [19, 22] and had been proved to be the dominant facet on CuO based catalysts [18]. In the current work, we performed systematic density functional theory (DFT) calculations of the surface structural properties of the reduced CuO(111) surface ($CuO_{1-x}$(111)) and its activity to oxidize CO. Our results showed that the charge transfer between the CO and $Cu^+$ caused by the electron localization enhanced the interaction between them, and the reduction degree of $CuO_{1-x}$(111) was found to be a very important factor for the CO oxidation.

## Computational details

All calculations were carried out using the Vienna ab initio simulation package (VASP) [24, 25]. The core-valence electron interaction was treated by using the project-augmented wave (PAW) [26, 27] method. The Perdew, Burke, and Ernzerhof (PBE) [28] functional within the generalized gradient approximation (GGA) was employed to evaluate the electronic exchange and correlation energy. Since the bulk CuO has an antiferromagnetic ground state, the spin polarized calculations were performed. The calculations were also conducted involving on-site Coulomb corrections (DFT+U) [29, 30] to describe the strong correlation effect among the partially filled Cu 3d states in CuO. The values of U=7 eV and J=0 eV for CuO were adopted, as suggested by Elliott et al. [22] and Nolan et al. [31]. The copper 3d, 4s, and the carbon and oxygen 2s, 2p electrons were treated as valence electrons. For bulk CuO, a Monkhorst-Pack [32] grid of 11×11×11 k-points was used, and the energy cutoff of plane wave expansion was set to 450 eV. For the surface slab, we used a 2×2 supercell, with a 400 eV cutoff energy and a Monkhorst-Pack grid of 1×1×1 k-points because of the large size of the slab (~11×12 $Å^2$). The slab thickness was six layers (~12 Å), with a 15 Å vacuum gap. For all structural optimizations, the bottom two layers were fixed, while the other layers were allowed to relax until the atomic forces reached below 0.05 eV/Å. The nudged elastic band (NEB) method was used to determine the transition states (TS) along the reaction pathways [33–38].

To estimate the adsorption energies of CO, the following equation was used,

$$E_{ads} = -(E_{slab+CO} - nE_{CO} - E_{slab})/n \quad (1)$$

where $E_{slab+CO}$ is the total energy of the system involving the slab with the adsorbed CO, $E_{CO}$, and $E_{slab}$ are energies of the gas-phase CO molecule and the surface slabs, respectively, n is the number of adsorbed CO molecules.

To estimate the binding energies of CO, the following equation was used,

$$E_{bind} = -(E^{fix}_{slab+CO} - nE_{CO} - E_{slab})/n \quad (2)$$

where $E^{fix}_{slab+CO}$ is the total energy of the system involving the fixed slab with the adsorbed CO, $E_{CO}$, and $E_{slab}$ are energies of the gas-phase CO molecule and the surface slabs, respectively, n is the number of adsorbed CO molecules.

## Results and discussion

The structural parameters of bulk CuO were optimized by using DFT+U method with the chosen parameters (U=7 eV

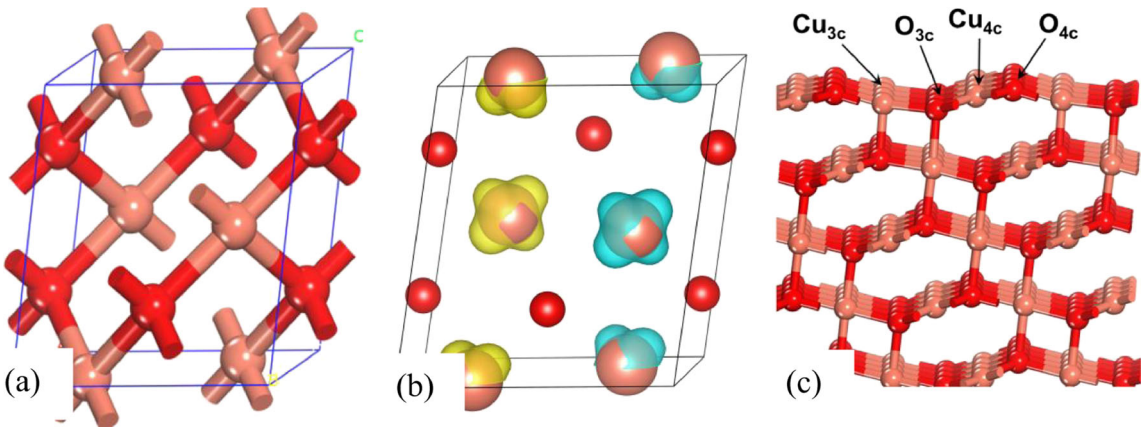


**Fig. 1** Calculated structures of CuO bulk and CuO(111) surface. (**a**) Structure of CuO bulk. (**b**) The isosurface (0.03 e/$Å^3$) of calculated spin charge densities, the yellow and blue denote spin up and down respectively. (**c**) Structure of CuO(111), different surface species are labeled. The Cu and O atoms are represented by balls in pink and red, respectively. The notation is used throughout this paper

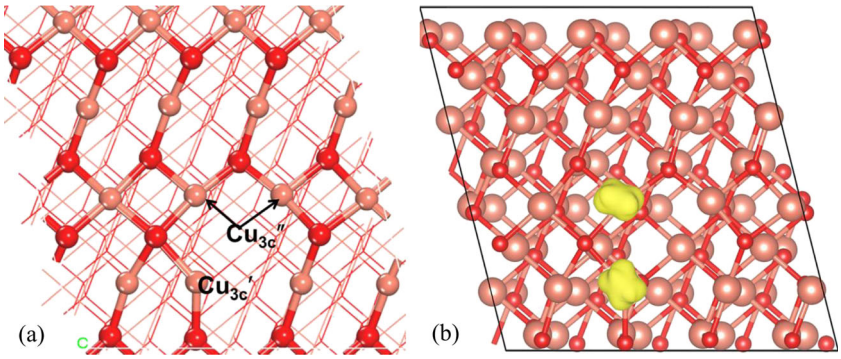


**Fig. 2** Top view of (**a**) calculated $CuO_{1-x}(111)$ containing one $O_{3c}$ vacancy and (**b**) corresponding localized spin density structure

and J=0 eV). The calculated lattice parameters are a=4.604 Å, b=3.485 Å, c=5.097 Å, β=99.6°, in good agreement with previous calculations [22] and the experiment values [39]. Figures 1(a) and (b) show the bulk structure and the isosurface (0.03 e/Å$^3$) of calculated antiferromagnetic spin charge densities. The calculated magnetic moment per Cu atom is 0.63 $\mu_B$, which is consistent with previous calculations [19, 22] and experiment measurements [40]. This suggests that the DFT+U approach and the U and J parameters are appropriate for the description of the CuO bulk. Therefore, we adopted the same values of U and J for surface calculations.

A representative structure of CuO(111) surface is illustrated in Fig. 1(c). Both fully saturated 4(4)-fold O(Cu) and coordinatively unsaturated 3(3)-fold O(Cu) are exposed on the surface, which are represented by $O_{4c}$, $Cu_{4c}$, $O_{3c}$, and $Cu_{3c}$, respectively. We first tested the CO adsorption at the pure CuO(111) surface, and got the most stable adsorption configuration as well as the adsorption energy (0.51 eV). Similar with the previous studies, this adsorption energy was so small that limited the CO oxidation activity. We then proceeded with the study of CO adsorption at reduced $CuO_{1-x}(111)$ surfaces.

## CO adsorption on $Cu^+$ and $Cu^{2+}$ sites

One usual way to reduce the CuO(111) surface is to remove one surface $O_{3c}$, thereby creating an oxygen vacancy ($O_v$). The calculated $CuO_{1-x}(111)$ surface with one $O_{3c}$ vacancy is shown in Fig. 2(a), together with the electronic structure (Fig. 2(b)). As one can see, with the formation of oxygen vacancy, one three-fold copper turned into a new three-fold copper ($Cu_{3c}'$), and two four-fold coppers on the surface became three-fold copper ($Cu_{3c}''$) due to the relaxation of the surface. Introducing one O vacancy gives rise to two excess electrons and they are localized on $Cu_{3c}'$ and one of the $Cu_{3c}''$ atoms close to the $O_v$ at the surface (Fig. 2(b)). The Bader charge analyses showed that both three-fold coordinated Cu atoms owned more charge than their counterparts on the surface (about 9.98 e), and calculated charges are 10.43 e and 10.35 e at $Cu_{3c}'$ and $Cu_{3c}''$, respectively (Table 1). Compared with the Bader charge of $Cu^+$ (10.39 e) in bulk $Cu_2O$, these two Cu ions should be considered the $Cu^+$, while the other Cu ions were still $Cu^{2+}$.

CO adsorption at $CuO_{1-x}(111)$ surface with one $O_{3c}$ vacancy ($O_v$) was calculated at different surface sites (Fig. 3(a-c)). As one may expect from the adsorption structures, the relaxation of the different surface sites were rather different. Significant relaxation occurred on $Cu_{3c}'$ and $Cu_{3c}''$, while that on $Cu^{2+}$ was rather tiny. According to our calculations, $Cu_{3c}'$ gives the strongest adsorption (Table 1). The adsorption energy is 1.31 eV on it, while it is 0.63 eV on $Cu_{3c}''$ and only 0.47 eV on $Cu^{2+}$. The bonding strengths of CO on both the $Cu^+$ sites ($Cu_{3c}'$, $Cu_{3c}''$) are higher than that on the $Cu^{2+}$ site of reduced and clean CuO(111) surface (0.51 eV). However, as one can see, the difference of CO adsorption energies between $Cu_{3c}'$ and $Cu_{3c}''$ is also quite dramatic.

In order to explain this discrepancy, we first calculated the relaxation of each Cu cation ($Cu_{3c}'$, $Cu_{3c}''$, and $Cu^{2+}$) caused by CO adsorption by measuring the corresponding root-mean-square (RMS) of displacements [41]:

$$r_{RMS} = \sqrt{\frac{1}{3}\sum_{i=1}^{3}\left(r_i - r_i^0\right)^2}$$

where $r_i^0$ and $r_i$ are the lengths of the three Cu-O bonds of each Cu (see Table S1 in Supporting information) before and after relaxation, respectively. The calculated $r_{RMS}$ for these Cu sites are listed in Table 1. It can be clearly seen that the larger the $r_{RMS}$ the bigger the adsorption energy of CO, indicating that the adsorption strength is related to the surface relaxation. However, they are not in linear correlation, in other words, it can be predicted that the surface relaxation does not seem to be the

**Table 1** Calculated Bader charge (e) and $r_{RMS}$ (Å) of different surface Cu cations ($Cu_{3c}'$, $Cu_{3c}''$, and $Cu^{2+}$) at $CuO_{1-x}(111)$ and average adsorption energies ($E_{ads}$, eV) and binding energies ($E_{bind}$, eV) of CO at these sites

| Site | Bader charge | $r_{RMS}$ | $E_{ads}$ | Figure | $E_{bind}$ | Figure |
|---|---|---|---|---|---|---|
| $Cu_{3c}'$ | 10.43 | 0.422 | 1.31 | 3(a) | 0.68 | S1(a) |
| $Cu_{3c}''$ | 10.35 | 0.325 | 0.63 | 3(b) | 0.23 | S1(b) |
| $Cu^{2+}$ | 9.94 | 0.045 | 0.47 | 3(c) | 0.17 | S1(c) |

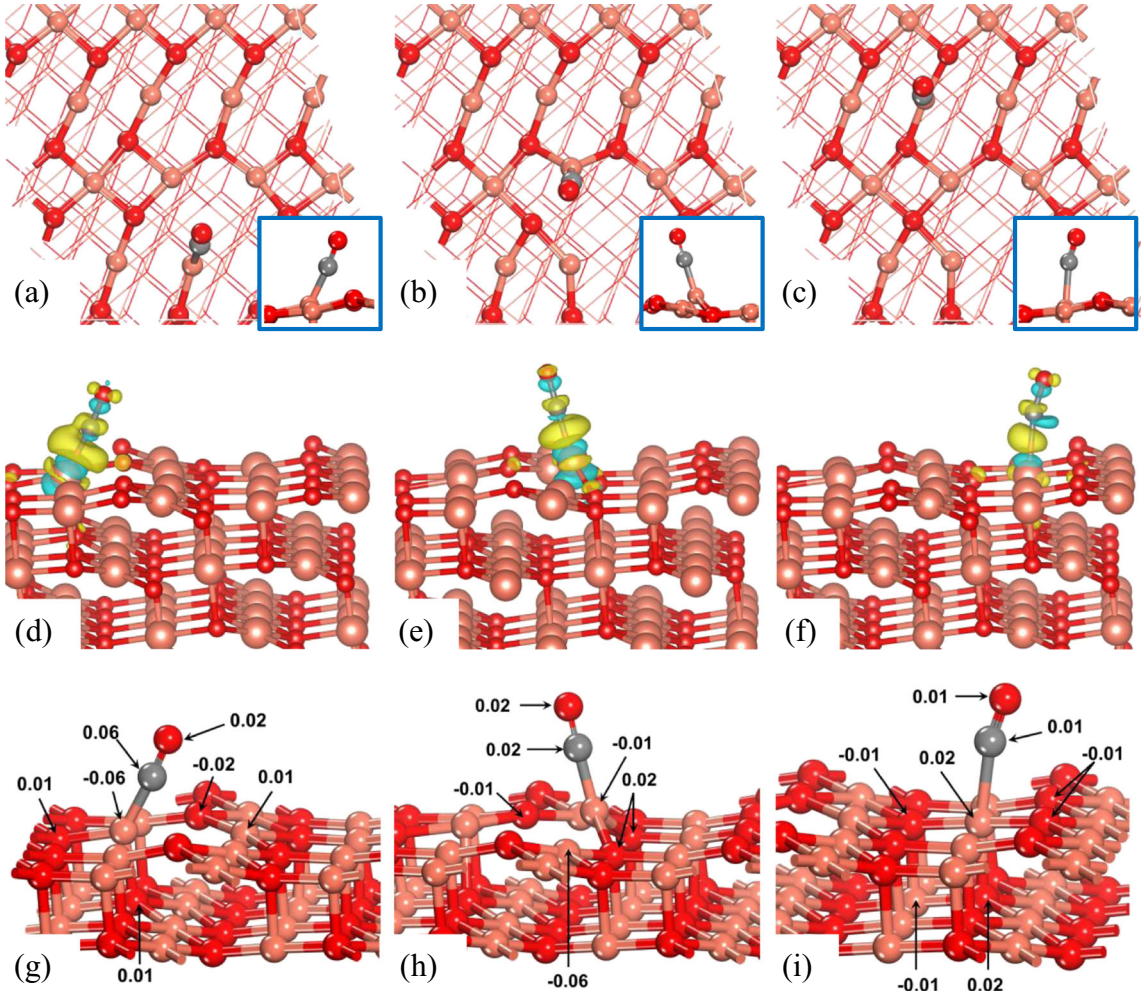


**Fig. 3** Calculated structures of CO adsorption at $CuO_{1-x}(111)$ with one $O_v$. (**a**)-(**c**): top view of one CO adsorbs at $Cu_{3c}'$, $Cu_{3c}''$ and $Cu^{2+}$ sites, respectively; (**d**)-(**f**): isosurfaces (0.004 e/Å$^3$) of charge redistribution of (**a**)-(**c**), respectively; (**g**)-(**i**): Bader charges of (**a**)-(**c**), respectively. The yellow and blue isosurfaces denote charge gain and miss, respectively. Positive and negative signs of Bader charges are for gain and lose of electrons. The gray balls denote C atoms

sole determining factor for the difference of CO adsorption strengths. We then calculated the charge density difference (Fig. 3(d-f)) and also performed the Bader charge analysis (Fig. 3(g-i)). The results showed that all the adsorbed CO molecules gain charge from the substrates, by as much as 0.08 e at $Cu_{3c}'$ site, 0.04 e at $Cu_{3c}''$ site and only 0.02 e at $Cu^{2+}$ site, respectively. As we can see, the charge transfer at $Cu_{3c}'$ site are more significant than that at $Cu_{3c}''$ and $Cu^{2+}$ sites, which are comparable. Considering the calculated irregular $r_{RMS}$ of them, the electronic interaction should be an important factor for the

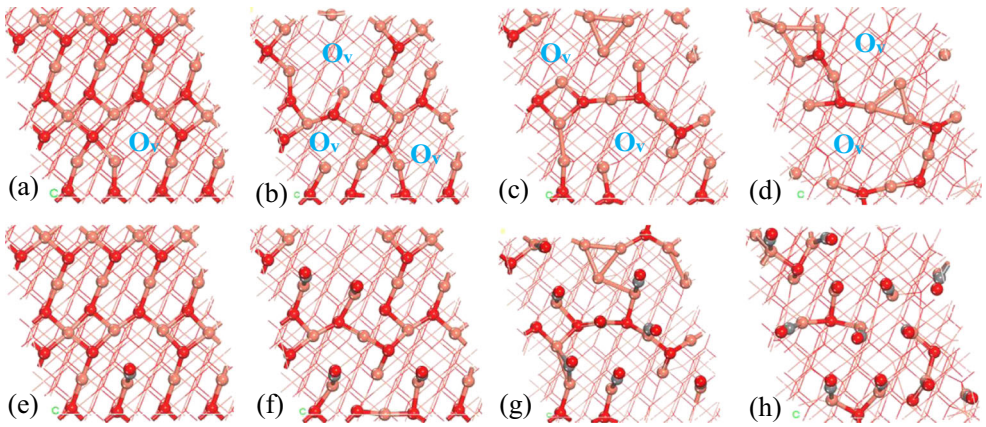


**Fig. 4** Calculated structures (top view) of $CuO_{1-x}(111)$ in different degrees of surface reduction, and corresponding adsorption structures of CO. (a, e) θ=6.25 %; (b, f) θ=25 %; (c, g) θ=50 %; (d, h) θ=75 %

**Table 2** Calculated average adsorption energies of CO at $CuO_{1-x}(111)$ in different degrees of surface reduction

| θ | $E_{ads}$ /eV | Figure |
|---|---|---|
| 0 | 0.51 | / |
| 6.25 % | 1.31 | 4(e) |
| 25 % | 1.18 | 4(f) |
| 50 % | 1.16 | 4(g) |
| 75 % | 1.05 | 4(h) |

large discrepancy of CO adsorption energies between $Cu_{3c}'$ and $Cu_{3c}''$, as well as the small difference between $Cu_{3c}''$ and $Cu^{2+}$.

To further verify the above explanation, we calculated the adsorption of CO on $Cu_{3c}'$, $Cu_{3c}''$ and $Cu^{2+}$ sites, with all atoms of $CuO_{1-x}(111)$ surface fixed to eliminate the influence of surface relaxation (see Fig. S1 in Supporting information). As we can see from Table 1, the binding energies of CO on $Cu_{3c}''$ and $Cu^{2+}$ sites are very similar. However, for $Cu_{3c}'$, it gives much higher binding energy (0.68 eV) than that of $Cu_{3c}''$ (0.23 eV) and $Cu^{2+}$ (0.17 eV). The trend of binding energies and adsorption energies are very similar. While the adsorption energies are always larger, because they include not only the binding energy but also the relaxation energy of the surface. Between sites $Cu_{3c}'$ and $Cu_{3c}''$, the binding energy difference is 0.45 eV and relaxation energy difference is 0.23 eV, together they make the adsorption energy difference to be 0.68 eV. That is to say, the binding energy is a more dominating factor than surface relaxation in determining the overall trends of CO adsorption energy.

## CO adsorption on $CuO_{1-x}$ (111) with different surface reduction degrees

The surface reduction degree of the $CuO_{1-x}(111)$ surface was calculated as follows: $\theta=N_{Ov}/N_O$, in which $N_{Ov}$ and $N_O$ are the numbers of oxygen vacancy and lattice oxygen on the top layer of surface slab, respectively. There are 16 lattice O atoms including eight $O_{3c}$ and eight $O_{4c}$ on CuO(111) surface. Herein this work, we just studied the typical reducing structures with the surface oxygen atoms removed, without considering the migration of $O_v$ to subsurface.

**Table 3** Reaction barriers of CO react with $O_{3c}$ and $O_{4c}$ atoms ($E_{a1}$, $E_{a2}$), and the numbers of $O_{3c}$ and $O_{4c}$ atoms ($N_1$, $N_2$), as well as the reaction activities (α) of $CuO_{1-x}(111)$ surfaces

| Term | Reduction degree (θ) / % | | | | |
|---|---|---|---|---|---|
| | 6.25 | 25 | 50 | 75 | 100 |
| $N_1$ | 1 | 4 | 2 | 2 | 0 |
| $N_2$ | 0 | 0 | 6 | 2 | 0 |
| $E_{a1}$ | 0.51 | 0.51 | 0.51 | 0.51 | 0 |
| $E_{a2}$ | 0 | 0 | 0.87 | 0.87 | 0 |
| α | 1.96 | 7.84 | 10.82 | 6.22 | 0 |

We calculated the stability of different surface structures of $CuO_{1-x}(111)$ in different degrees of surface reduction (see Figs. (S2-S4)), and for the surface reduction degree of 6.25 %, 25 %, 50 %, and 75 %, the most stable surface structures are presented in Fig. 4. For θ=25 %, four $O_{3c}$ atoms were removed (Figs. 4(b) and S2(b)), while for θ=50 %, six $O_{3c}$ and two $O_{4c}$ atoms were removed (Figs. 4(c) and S3(b)), and for θ=75 %, six $O_{3c}$ and six $O_{4c}$ atoms were removed (Figs. 4(d) and S4(b)). As we can see, for $CuO_{1-x}(111)$ with high reduction degree, the surfaces distorted seriously. With the decrease of surface lattice oxygen, excess electrons as well as the unsaturated Cu atoms increased. As we studied above, $Cu^+$ species which are reduced by the excess electrons give rise to the strong adsorption of CO at the surface. So we calculated the structures of CO molecules adsorbed on the $Cu^+$ sites (Fig. 4(e-h)), which are proved to be the most stable adsorption sites ($Cu_{3c}'$) in the above section. The number of adsorbed CO molecules is consistent with the number of the oxygen atoms which are removed on the surface.

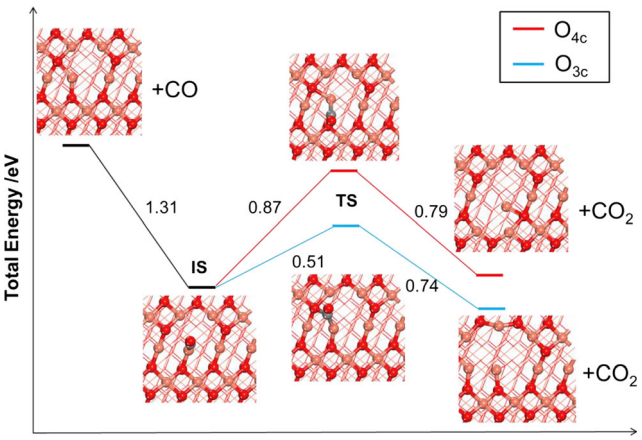


**Fig. 5** Energy profiles of CO oxidation by (blue) three- and (red) four-coordinated oxygen at reduction surfaces of $CuO_{1-x}(111)$. The $CO_2$ adsorption state is not plotted in the profiles for clarity

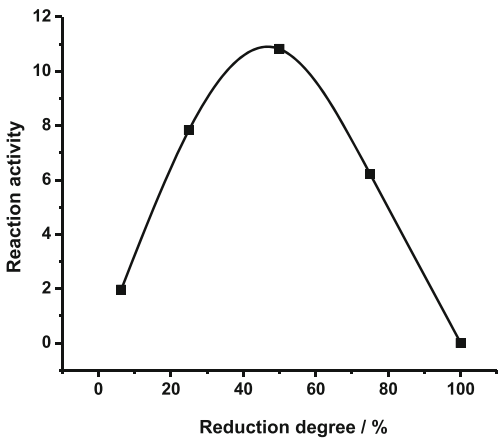


**Fig. 6** Relationship between reaction activity and reduction degree on $CuO_{1-x}(111)$ surface

From the calculated adsorption energies, which are listed in Table 2, we can see that the reduced $CuO_{1-x}(111)$ surfaces all give much stronger adsorption compared to the pure surface and the average adsorption energies are all above 1 eV. These results give us a clear indication that the greater the surface reduction, the larger the amount of CO that can be stably adsorbed, and the larger probability that it is oxidized. In addition to the coverage of CO on the surface, the amount of lattice O that can participate in the reaction as well as the reaction energy barrier are also important factors for the CO oxidation rate.

We then studied the CO oxidation at the $Cu^+$ site of $CuO_{1-x}(111)$ with $\theta=6.25$ %, and the reaction pathway is plotted in Fig. 5. It has been found that CO can adsorb at this site with the adsorption energy of 1.31 eV. The energy barriers for CO react with the $O_{4c}$ and $O_{3c}$ were estimated to be 0.87 eV and 0.51 eV, respectively. Both of these energy barriers are relatively low for CO oxidation. In other words, the reaction activity of CO on reduced $CuO_{1-x}(111)$ surface should be high as long as the surface lattice oxygen are adequate. In this sense, one may expect that, with the increase of the surface reduction degree, the activity of CO oxidation at $CuO_{1-x}(111)$ surface first raises and then declines, because the lattice oxygen at highly reduced surface are severely inadequate. In fact, this trend has been confirmed by Ye and coworkers in their experimental studies [18], that the CuO based catalysts with a certain reduction degree (≈ 77 %) gives the highest activity.

To obtain a general understanding of the amount of lattice oxygen and energy barrier for CO oxidation quantitatively, we calculated the reaction activity ($\alpha$) as a function of them. As is known to us, that the energy barrier is opposite to reaction activity, while the amount of lattice oxygen participated in the reaction is proportional to it. Accordingly, $\alpha$ can be written as follows: $\alpha=1/E_{a1}\cdot N_1+1/E_{a2}\cdot N_2$, in which $E_{a1}$ and $E_{a2}$ are the energy barriers for CO react with $O_{3c}$ and $O_{4c}$ atoms at $CuO_{1-x}(111)$ with $\theta=6.25$ %, and $N_1$ and $N_2$ are the numbers of $O_{3c}$ and $O_{4c}$ that left on the surface to react with CO, respectively. In Table 3, we list the calculated reaction activity and the corresponding parameters for different reduction degrees of $CuO_{1-x}(111)$ surface. It needs to be mentioned that when the reduction degree is relatively low, the number of $O_{3c}$ is larger than that of CO, and CO will react only with $O_{3c}$ rather than $O_{4c}$, so $E_{a2}$ was considered to be zero. Yet, when the reduction degree is high, say 50 % and 75 % (see Table 3), the number of CO is adequate enough to react both with $O_{3c}$ and $O_{4c}$, when $E_{a1}$ and $E_{a2}$ should not be considered as zero. Nevertheless, when the surface is absent of oxygen, there will be no reaction at all. As one can see, the reaction activity presents the obvious trends that fist increased and then decreased, which are also shown in Fig. 6. The highest activity for CO oxidation at reduced $CuO_{1-x}(111)$ surface as we fit is approximately 50 %, which is not completely consistent with the experimental results. The reason may be the migration of oxygen vacancy from the surface to the subsurface or deeper in the bulk which makes our model to consider the reaction activity very complicated and we may tackle this issue in future work.

## Conclusions

In summary, by systematically performing DFT calculations with the correction of on-site Coulomb interactions, we have studied the adsorption and reaction of CO at reduced $CuO_{1-x}(111)$ with different reduction degrees. According to our calculation results, CO gives much higher adsorption energies on $Cu^+$ sites than that on $Cu^{2+}$ site of $CuO_{1-x}(111)$, and its adsorption strength is related to the electronic interaction with the substrate as well as the structural relaxation. In particular, the electronic interaction is proved to be the decisive factor for the difference of CO adsorption energies at these sites by calculating the $r_{RMS}$ of the corresponding sites and $E_{bind}$ of CO. Moreover, the calculated reaction activity of CO react with the lattice oxygen on reduced $CuO_{1-x}(111)$ first increases then declines, consistent with the experiment results.

**Acknowledgments** This work was supported by the Plan of Shanghai City Outstanding Technical Leaders (12XD1421700), Innovation Program of Shanghai Municipal Education Commission (12YZ161), Natural Science Foundation of Shanghai (15ZR1421500), and Science and Technology Innovation project of Shanghai Putuo District (2014Q001A).

## References

1. Royer S, Duprez D (2011) Chem Cat Chem 3:24–65
2. Huang TJ, Tsai DH (2003) Catal Lett 87:73–178
3. Chon H, Prater CD (1966) Faraday Soc 41:380–393
4. Moretti E, Lenarda M, Storaro L, Talon A, Frattini R, Polizzi S, Rodríguez-Castellón E, Jiménez-López A (2007) Appl Catal B Environ 72:149–156
5. Hasegawa Y, Fukumoto K, Ishima T, Yamamoto H, Sano M, Miyake T (2009) Appl Catal B Environ 89:420–424
6. Ayastuy JL, Gurbani A, González-Marcos MP, Gutiérrez-Ortiz MA (2010) Appl Catal A Gen 387:119–128
7. Fan XL, Liu Y, Du XJ, Liu C, Zhang C (2013) Acta Phys -Chim Sin 29:263–270
8. Luo MF, Song YP, Lu JQ, Wang XY, Pu ZY (2007) J Phys Chem C 111:12686–12692
9. Skårman B, Grandjean D, Benfield RE, Hinz A, Andersson A, Wallenberg LR (2002) J Catal 211:119–133
10. Rao KN, Bharali P, Thrimurthulu G, Reddy BM (2010) Catal Commun 11:863–866
11. Martínez-Arias A, Fernández-García M, Gálvez O, Coronado JM, Anderson JA, Conesa JC, Soria J, Munuera G (2000) J Catal 195: 207–216
12. Hornés A, Hungría AB, Bera P, Cámara AL, Fernández-García M, Martínez- Arias A, Barrio L, Estrella M, Zhou G, Fonseca JJ, Hanson JC, Rodriguez JA (2010) J Am Chem Soc 132:34–35

13. Jia AP, Jiang SY, Lu JQ, Luo MF (2010) J Phys Chem C 114: 21605–21610
14. Jia AP, Hu GS, Meng L, Xie YL, Lu JQ, Luo MF (2012) J Catal 289:199–209
15. Lee HC, Kim DH (2008) Catal Today 132:109–116
16. Avgouropoulos G, Ioannides T, Matralis H (2005) Appl Catal B Environ 56:87–93
17. Wan H, Wang Z, Zhu J, Li X, Liu B, Gao F, Dong L, Chen Y (2008) Appl Catal B Environ 79:254–261
18. Ye LP, Zhan JR, Zhang R, Sun YJ, Li JL, Wu XY, Luo Y (2012) Fine Chemicals 29:1066–1071
19. Hu J, Li DD, Lu JG, Wu RQ (2010) J Phys Chem C 114:17120–17126
20. Polster CS, Nair H, Bacrtsch CD (2009) J Catal 266:308–319
21. Wang HF, Kavanagh R, Guo YL, Guo Y, Lu GZ, Hu P (2012) J Catal 296:110–119
22. Maimaiti Y, Nolan M, Elliott SD (2014) Phys Chem Chem Phys 16: 3036–3046
23. Bao HZ, Zhang WH, Hua Q, Jiang ZQ, Yang JL, Huang WX (2011) Angew Chem Int Ed 50:12294–12298
24. Kresse G, Furthmüller J (1996) Comput Mater Sci 6:15–50
25. Kresse G, Furthmüller J (1996) Phys Rev B 54:11169–11186
26. Kresse G, Joubert D (1999) Phys Rev B 56:1758–1775
27. Blöchl PE (1994) Phys Rev B 50:17953–17979
28. Perdew JP, Burke K, Ernzerhof M (1996) Phys Rev Lett 77:3865–3868
29. Dudarev SL, Botton GA, Savrasov SY, Humphreys CJ, Sutton AP (1998) Phys Rev B 57:1505–1509
30. Anisimov VI, Aryasetiawan F, Lichtenstein AI (1997) J Phys Condens Matter 9:767–808
31. Nolan M, Elliott SD (2006) Phys Chem Chem Phys 8:5350–5358
32. Monkhorst HJ, Pack JD (1976) Phys Rev B 13:5188
33. Jonsson H, Mills G, Jacobsen KW (1998) Nudged elastic band method for finding minimum energy paths of transitions. World Scientific, Singapore
34. Henkelman G, Jónsson H (2000) J Chem Phys 113:9978–9985
35. Henkelman G, Uberuaga BP, Jónsson H (2000) J Chem Phys 113: 9901–9904
36. Sheppard D, Terrell R, Henkelman G (2008) J Chem Phys 128: 134106
37. Sheppard D, Henkelman G (2011) J Comput Chem 32:1769–1771
38. Sheppard D, Xiao P, Chemelewski W, Johnson DD, Henkelman G (2012) J Chem Phys 136:074103
39. Åsbrink S, Norrby LJ (1970) Acta Crystallogr Sect B: Struct Sci 26: 8–15
40. Yang BX, Thurston TR, Tranquada JM, Shirane G (1989) Phys Rev B: Condens Matter Mater Phys 39:4343–4349
41. Wang HF, Gong XQ, Guo YL, Guo Y, Lu GZ, Hu P (2009) J Phys Chem C 113:10229–10232